

Miyamoto et al.

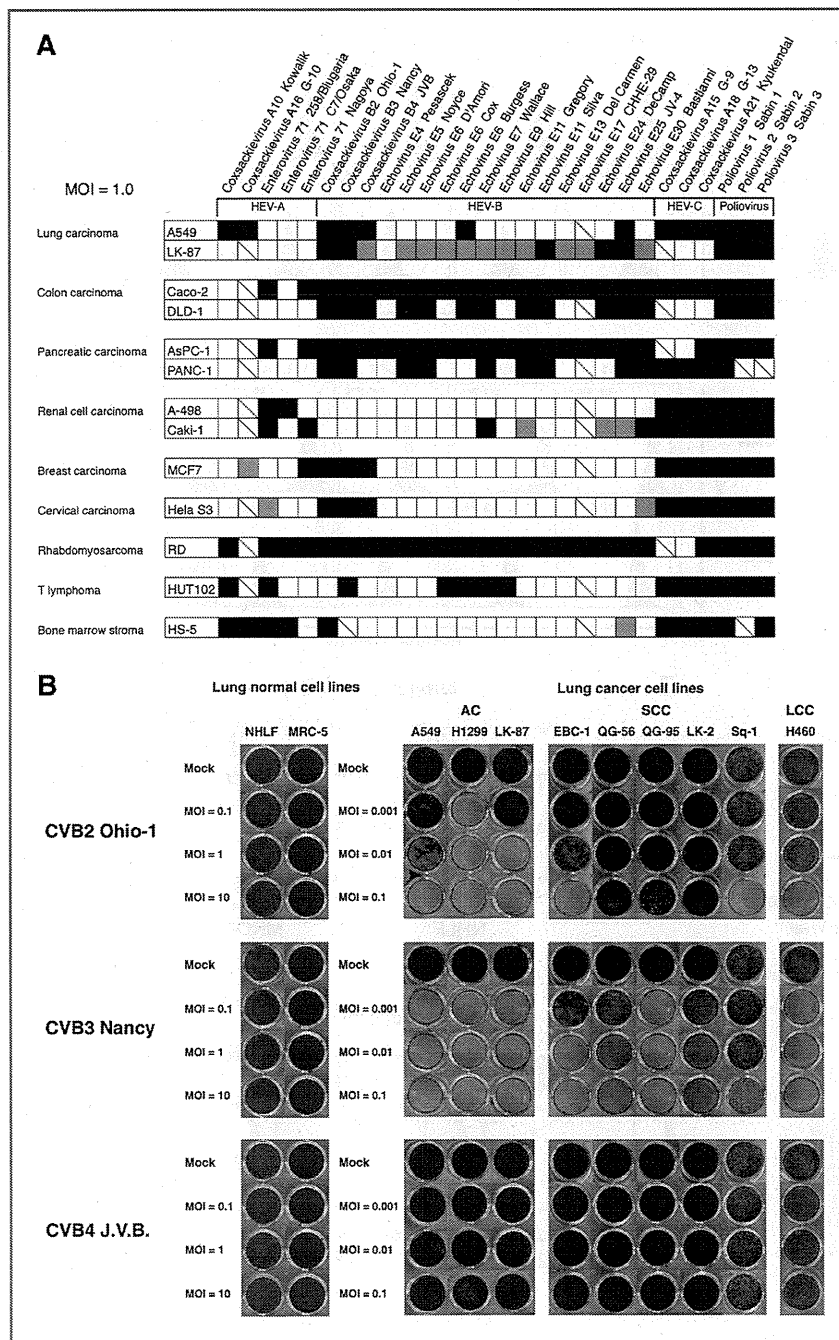


Figure 1. Sequential 2-step screenings to identify a potent oncolytic virus candidate. A, various cancer cell lines and HS-5 cells were infected with 28 strains of enterovirus at an MOI of 1.0 and incubated for 1 hour. At 72 hours postinfection, cell viability was assessed by crystal violet staining. Black, gray, white, and hashed boxes indicate greater than 50% cytotoxicity, less than 50% cytotoxicity, no cytotoxicity, and not analyzed, respectively. HEV-A, human enterovirus A; HEV-B, human enterovirus B; HEV-C, human enterovirus C. B, various human NSCLC and normal lung cell lines were infected with CVB2, CVB3, and CVB4 for 72 hours at MOIs of 0.001, 0.01, and 0.1 for NSCLC cell lines and MOIs of 0.1, 1.0, and 10 for normal cell lines, respectively. Cell viability was assessed by crystal violet staining. AC, adenocarcinoma; SCC, squamous cell carcinoma; LCC, large cell carcinoma.

treated MRC-5 normal lung cells (Fig. 3A). We analyzed externalization of phosphatidylserine and DNA fragmentation, hallmarks of apoptosis. CVB3-treated A549 cells showed a greater proportion of apoptotic (AnnexinV⁺/7-AAD⁻) and necrotic (AnnexinV⁺/7-AAD⁺) cells than LK-2 cells, correlating with

CAR expression (Fig. 3B). Similarly, exposure of A549 cells to CVB3 induced more sub-G₁ cells with DNA fragmentation than LK-2 cells, correlating with CAR expression. In contrast, neither Annexin V positivity nor DNA fragmentation was induced in CVB3-treated MRC-5 cells (Fig. 3C). To determine whether

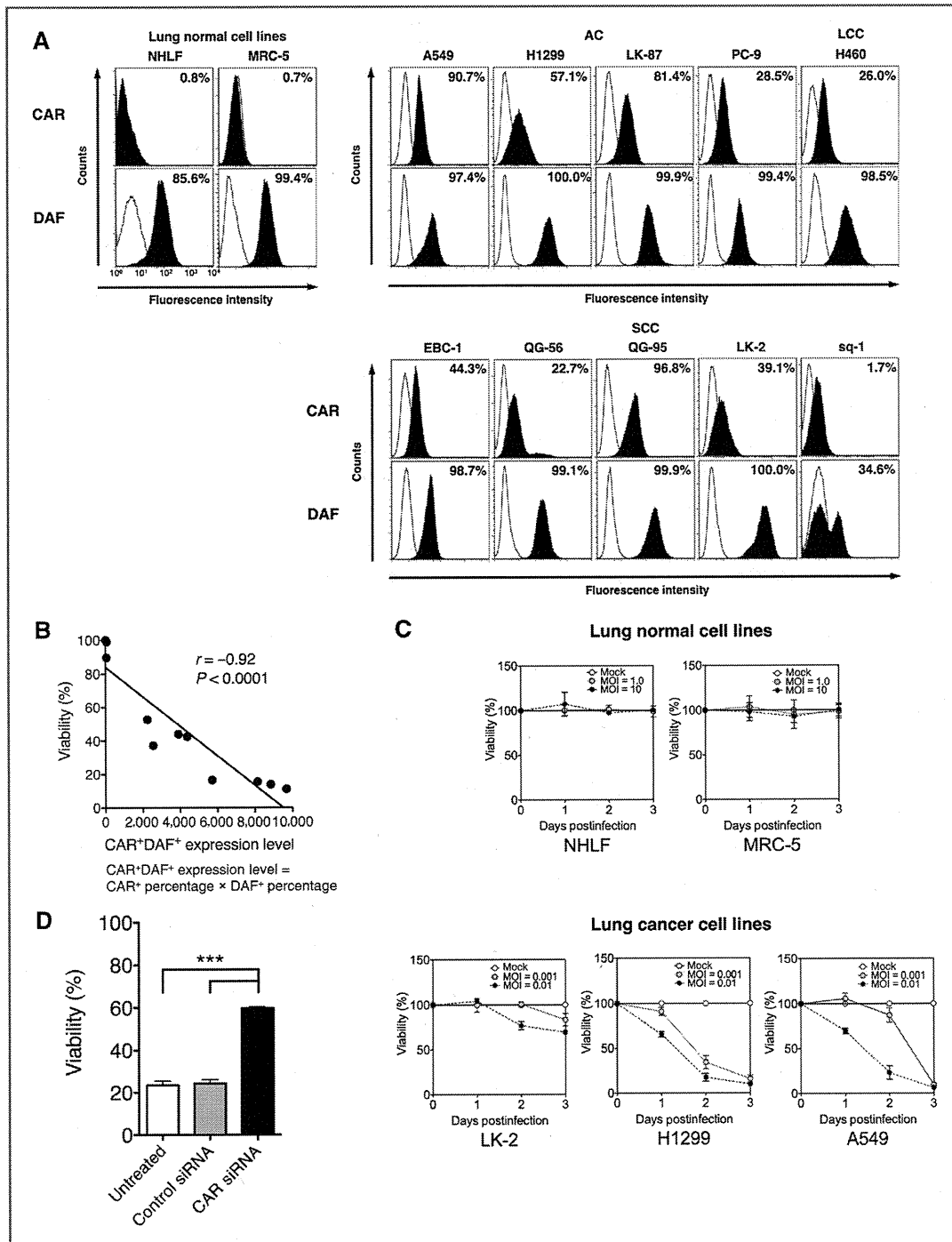


Figure 2. Expression profile of surface CAR and DAF on normal lung and NSCLC cells and its correlation with CVB3-mediated cytotoxicity. A, surface expression of CVB3 receptors on various lung cell lines was quantified by flow cytometry. Histograms represent the measured fluorescence of cells incubated with an isotype control antibody (unshaded) and anti-CAR or anti-DAF antibody (shaded). B, correlation between expression of CAR and DAF and cell viability at 72 hours after CVB3 infection ($r = -0.92$; $P < 0.0001$). C, cells infected with CVB3 at indicated MOIs was analyzed at indicated time points for cell viability by MTS assay. Each value was normalized to Opti-MEM-treated cells (mock) and represents the mean \pm SD. D, A549 cells transfected with CAR-specific siRNA or control siRNA were infected with CVB3 (MOI = 10), and assessed by MTS cell viability assay at 48 hours after CVB3 infection. Each value was normalized to mock and represents the mean \pm SD. ***, $P < 0.001$.

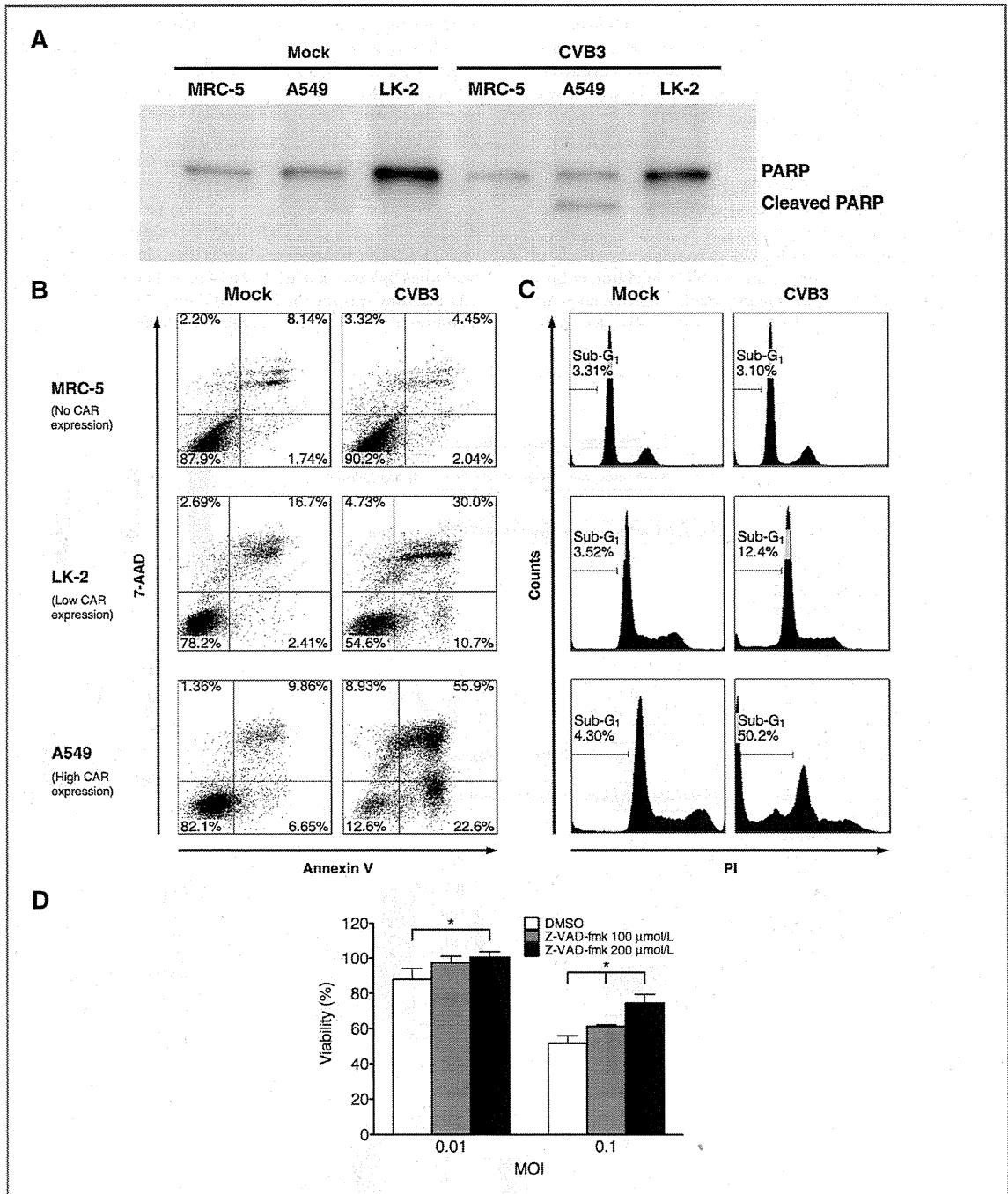


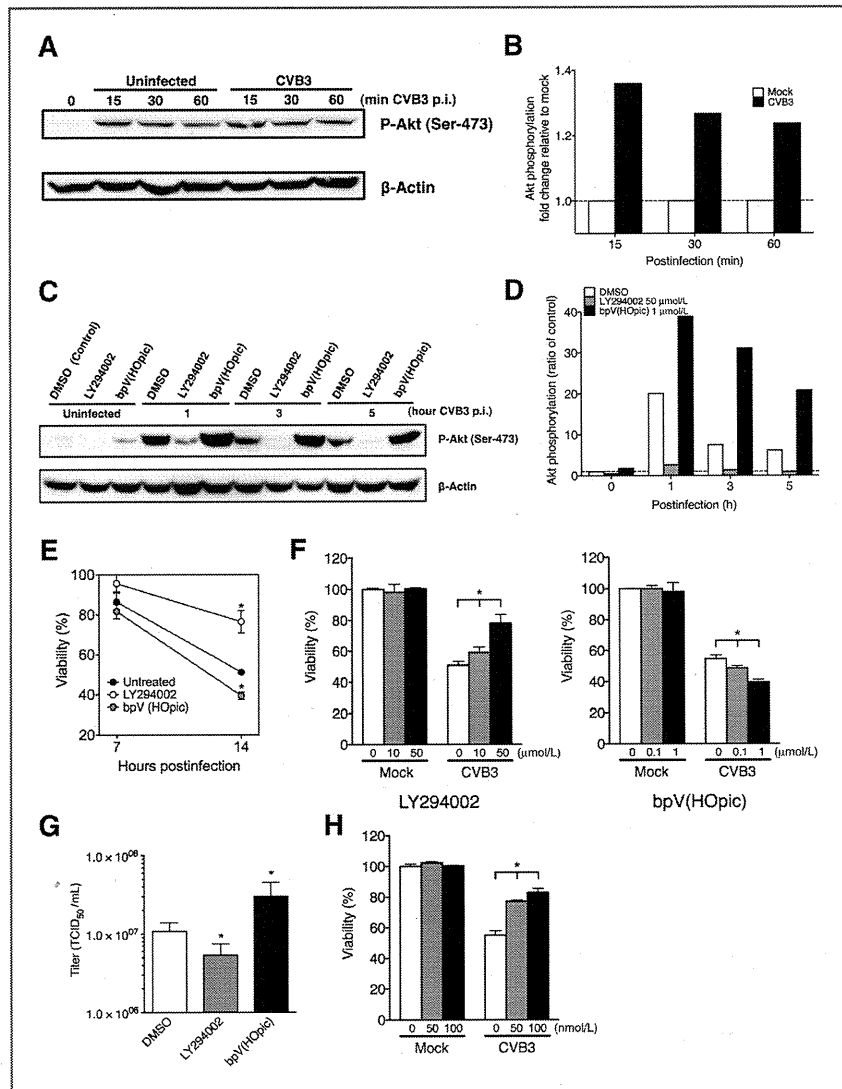
Figure 3. Correlation between caspase-dependent apoptosis and CVB3-mediated cytotoxicity in NSCLC cells. Lung cell lines infected with CVB3 (MOI = 0.1) were analyzed 24 hours later. A, each cellular lysate obtained was subjected to immunoblot analysis. Full-length PARP (116 kDa) and cleaved PARP (85 kDa) are shown. B, early apoptotic population was represented as Annexin V-PE⁺/7-AAD⁻ cells. C, each histogram PI depicts the population of cells in G₁ and G₂-M, and the apoptotic subdiploid peak (sub-G₁). D, cells pretreated with dimethyl sulfoxide (DMSO) or z-VAD-fmk and incubated with mock or CVB3 at indicated MOIs were subjected to MTS cell viability assays. *, *P* < 0.05.

CVB3-inducible apoptosis contributed to CVB3-mediated cytotoxicity against A549 cells, we treated them with the pan-caspase inhibitor, z-VAD-fmk. CVB3-mediated cytotoxicity was slightly but significantly reduced when z-VAD-fmk was added in a dose-dependent manner (Fig. 3D).

Because PI3K/Akt signaling pathways mediate CVB3 replication in human cancer cells (26), we investigated whether CVB3 infection could activate Akt phosphorylation (p-Akt) in A549 cells. CVB3 infection induced substantial p-Akt expression on the Ser-473 residue, peaking at 15 minutes postinfection (Fig. 4A and B), prompting us to examine the effects of pretreatment with LY294002, a specific PI3K inhibitor, or bpV, an inhibitor of PTEN that antagonizes PI3K activity, on p-Akt expression levels in CVB3-treated A549 cells. LY294002

reduced but bpV enhanced the level of p-Akt induced by CVB3 infection (Fig. 4C and D). In addition, LY294002 significantly diminished but bpV significantly augmented CVB3-mediated cytotoxicity against A549 cells at 14 hours after infection in a dose-dependent manner, whereas no cytotoxicity was observed when either of these agents were used in the absence of CVB3 (Fig. 4E and F). To unravel the relationship between p-Akt expression and CVB3 replication, we examined the effects of LY294002 or bpV on release of CVB3 progeny from CVB3-treated A549 cells. The CVB3 titer was significantly reduced when LY294002 was added, whereas it was increased almost 2-fold when bpV was added ($P < 0.05$; Fig. 4G), showing that PI3K/Akt pathway was involved in CVB3 replication. Furthermore, addition of a potent MEK inhibitor PD0325901, which blocks

Figure 4. Correlation between 2 survival signaling pathways and CVB3-mediated cytotoxicity and viral replication in human NSCLC cell lines. A549 cells infected with CVB3 (MOI = 0.1) were analyzed. A and B, each cell lysate collected at indicated time points was subjected to Western blotting assay for p-Akt on Ser-473 detection. Results normalized to mock were evaluated by densitometric analysis using Multi Gauge. C and D, p-Akt expression in A549 cells treated with LY294002 or bpV followed by CVB3 infection was determined by Western blotting analysis. E, A549 cells were treated with 50 $\mu\text{mol/L}$ LY294002, 1 $\mu\text{mol/L}$ bpV, or DMSO for 1 hour, infected with CVB3 or Opti-MEM for 1 hour, incubated for 7 or 14 hours, and subjected to MTS cell viability assays. *, $P < 0.05$. F, A549 cells treated as above were incubated for 14 hours at various concentrations of LY294002 or bpV and subjected to MTS cell viability assays. *, $P < 0.05$. G, supernatants from the LY294002- or bpV-treated A549 cells after 14 hours of CVB3 infection were collected and viral titer was determined. *, $P < 0.05$. H, A549 cells were treated with various concentrations of MEK inhibitor PD0325901 or DMSO for 1 hour, followed by CVB3 infection, incubated for 14 hours, and subjected to MTS cell viability assay. *, $P < 0.05$.



phosphorylation of ERK, to CVB3 infection significantly decreased cytotoxicity against A549 cells in a dose-dependent manner, whereas PD0325901 alone did not have any effect (Fig. 4H).

Efficacy studies in nude mice

We next evaluated *in vivo* oncolytic effects of CVB3 and its tolerability in nude mice bearing subcutaneous NSCLC xenografts. A single dose of intratumoral CVB3 administered into A549 xenografts significantly suppressed tumor growth ($P < 0.01$; Fig. 5A). In addition, the survival rate was significantly improved in CVB3-treated mice compared with untreated mice ($P = 0.0008$; Fig. 5B). To evaluate tolerability and dose-dependent oncolytic effects, 5 consecutive doses of CVB3 were intratumorally administered into A549 xenografts. The treatment with CVB3 elicited significant tumor regression in a dose-dependent manner ($P < 0.05$; Fig. 5C), with significantly prolonged survival ($P = 0.0004$). Moreover, half of the CVB3-treated mice achieved complete regression of the tumor (Fig. 5D). Similarly, in the EBC-1 human squamous cell carcinoma xenograft model, intratumoral 5 administrations of CVB3 revealed significant antitumor effects. All CVB3-treated mice achieved complete tumor elimination with a significantly prolonged survival rate (Fig. 5E and F). For H1299 human adenocarcinoma xenograft, similar potent antitumor effects with complete tumor rejection were observed in all of CVB3-treated mice (Supplementary Fig. S3). Notably, none of the mice died of side effects during these treatments.

To further investigate systemic oncolytic effects of CVB3, we used a mouse model with bilaterally preestablished subcutaneous A549 xenografts. Five consecutive CVB3 administrations into the right flank tumors only significantly suppressed the growth of both the CVB3-injected tumor and the distant untreated tumor when compared with untreated mice ($P < 0.05$; Fig. 5G), and displayed a significantly prolonged survival rate ($P = 0.0021$) and no lethality (Fig. 5H). To clarify the mechanism by which CVB3 exerted antitumor effects against the contralateral tumor, we investigated whether the supernatants derived from disrupted untreated tumors or from CVB3-treated tumors had oncolytic activity against A549 cells. The supernatants derived from both CVB3-treated and CVB3-untreated tumors destroyed A549 cells (Fig. 5I), showing that replication-competent CVB3 did exist in untreated contralateral tumors.

Immunologic assays

As preapoptotic exposure to CRT and ATP release and postapoptotic HMGB1 are required for immunogenic cell death induced by chemotherapeutic agents such as anthracyclines and oxaliplatin (18), we examined whether CVB3 infection promoted similar effects on NSCLC cells. CVB3 treatment induced abundant surface exposure of CRT (Fig. 6A) on both A549 and H1299 cells, and active secretion of extracellular ATP was in dose- and time-dependent manner (Fig. 6B). In addition, CVB3 infection resulted in substantial release of HMGB1, another determinant of immunogenicity, from the nuclei of both A549 and H1299 cells into the cytosol (Fig. 6C).

We next evaluated the effects of intratumoral CVB3 administration on tumor-infiltrating immune cells in A549-bearing mice. CVB3 administration recruited significantly greater accumulation of NK cells, granulocytes, macrophages, and DCs into the tumor bed compared with the controls ($P < 0.01$; Fig. 7A and B). The tumor-infiltrating DCs expressed significantly higher levels of the costimulatory molecules CD80, CD86, and the maturation marker CCR7 in CVB3-treated mice compared with untreated mice ($P < 0.05$; Fig. 7C). It has been reported that mobilized CD107a expression, a cytolytic degranulation marker, correlates with NK cell-mediated lytic potential (27), and that granulocytes contribute to the antitumor effect of the oncolytic measles virus (28). We therefore explored the effects of CVB3 treatment on tumor-infiltrating CD107a-harboring NK cells and granulocytes. A higher density of NK cells as well as granulocytes mobilized CD107a to their cell surface in CVB3-treated mice compared with untreated mice (Fig. 7D). We further investigated the role of endogenous NK cells or granulocytes on the CVB3-mediated antitumor effect by depleting tumor-bearing mice of NK cells or granulocytes. Depletion of either NK cells or granulocytes significantly abrogated the therapeutic effect of CVB3 ($P < 0.05$; Fig. 7E), illustrating their substantial contribution to CVB3-induced antitumor responses.

Discussion

Lung cancer is the world's leading cause of cancer death, resulting in more than 1 million deaths per year worldwide (29). However, standard conventional therapies have produced limited cures, highlighting the need to develop novel therapeutic modalities (30). Here, we successfully identified CVB3 as a useful virotherapeutic agent against NSCLC via large-scale screenings with 28 strains of human enteroviruses (Fig. 1).

Discriminatory mechanisms for selectively targeting cancer cells are a prerequisite for therapeutic oncolytic viruses. CVB3 possessed cancer-specific viral tropism, as evidenced by an extremely low infection of MOI = 0.001 (Fig. 1B). In addition, CVB3-induced cytotoxicity positively correlated with the expression levels of DAF and particularly CAR on NSCLC cells (Fig. 2). CAR is expressed on various histologic types of human lung cancers, but not on normal alveolar epithelial cells (31). DAF counteracts the cytolytic action of the complement system and whose expression is upregulated on the surface of many tumors, seems to be a good target for oncolytic virus (32). These findings form a basis for the use of CVB3 in therapeutic applications for NSCLC patients.

Our results showed a moderate contribution of caspase-mediated apoptosis to CVB3-mediated oncolysis in human NSCLC cells (Fig. 3D). Generally, a wide range of cancers are known to be resistant to apoptosis following chemotherapy (33). Thus, the ability of CVB3 to induce apoptosis is an attractive property for the treatments of refractory NSCLC (34, 35). A role of PI3K/Akt signaling in accelerating CVB3 replication in NSCLC cells was also shown by use of cotreatment with a PTEN inhibitor and CVB3 infection (Fig. 4F and G). Overexpression of p-Akt and loss of PTEN expression in NSCLC

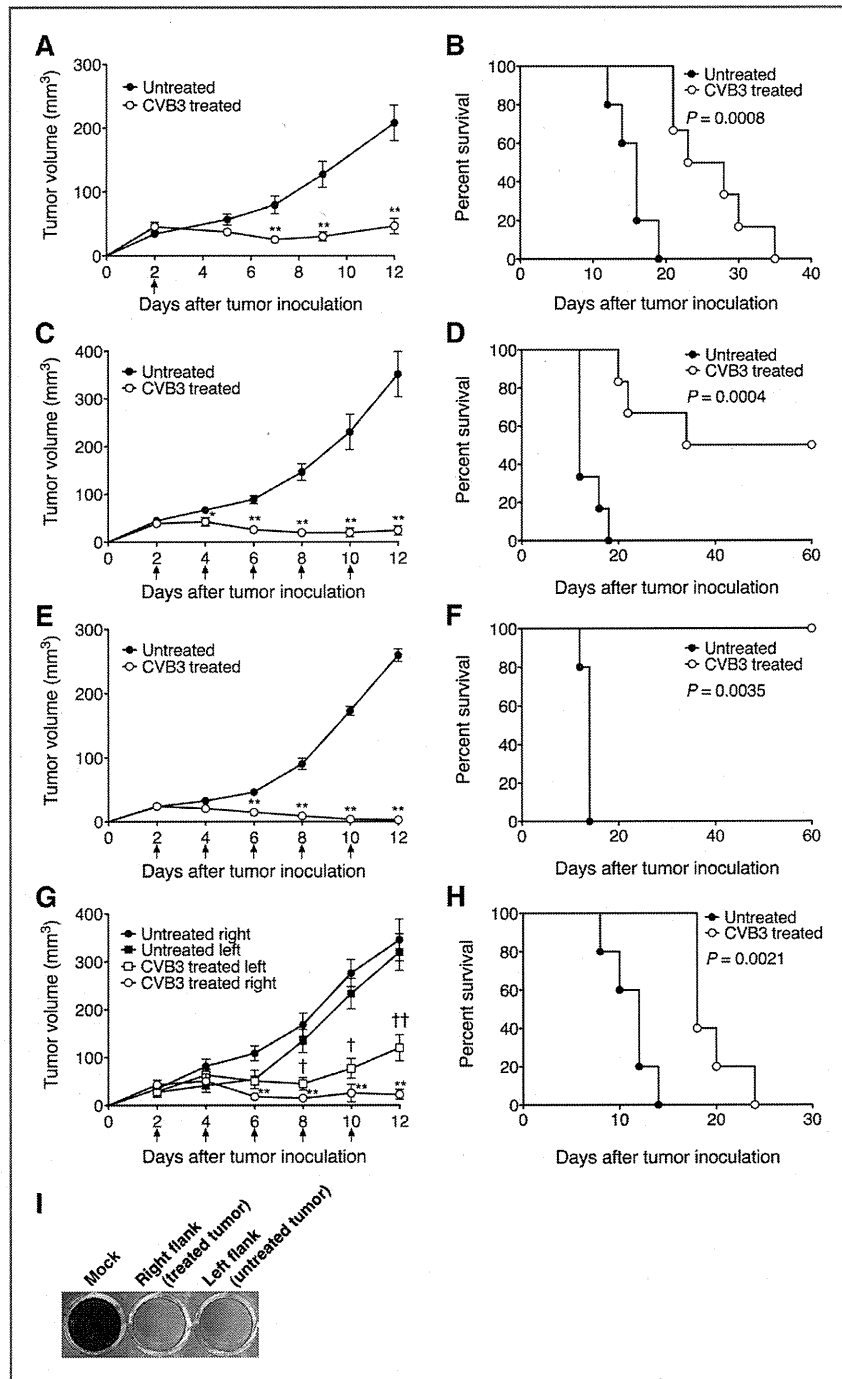


Figure 5. *In vivo* oncolytic effect of intratumoral CVB3 administration on various human NSCLC xenografts. A549 ($n = 5$ or 6; A and C) or EBC-1 ($n = 5$; E) were subcutaneously injected into the right flanks of nude mice. Each mouse received either a single dose (A), or 5 doses (C and E) of CVB3 intratumorally. Tumor volumes are expressed as means \pm SEM. *, $P < 0.05$; **, $P < 0.01$. Kaplan-Meier survival analyses are shown for CVB3-treated mice with the single dose (B; $P = 0.0008$) or 5 doses (D; A549, $P = 0.0004$; F; EBC-1, $P = 0.0035$) of the CVB3. G, administration of CVB3 to the right tumor was carried out to the nude mice with bilateral tumors ($n = 5$). *, $P < 0.05$; **, $P < 0.01$. Each symbol represents the statistical significance of right (*) and left (†) lateral tumors between untreated and CVB3-treated mice. H, Kaplan-Meier survival analyses of the mice in G are shown ($P = 0.0021$). I, two days after the CVB3 administration, the culture supernatants obtained from bilateral tumors were evaluated for oncolytic activity against cultured A549 cells.

patients was reported to confer poor differentiation, distant metastasis, and poor prognosis (36). In addition, PI3K/Akt pathway-related genes are frequently activated in diverse human cancers including NSCLC tumors (37), and cancer stem

cells after systemic chemotherapy (38, 39). These findings suggest that CVB3 treatment may be suitable for NSCLC patients refractory to conventional chemotherapies. In contrast, our finding that PI3K inhibition reduced CVB3

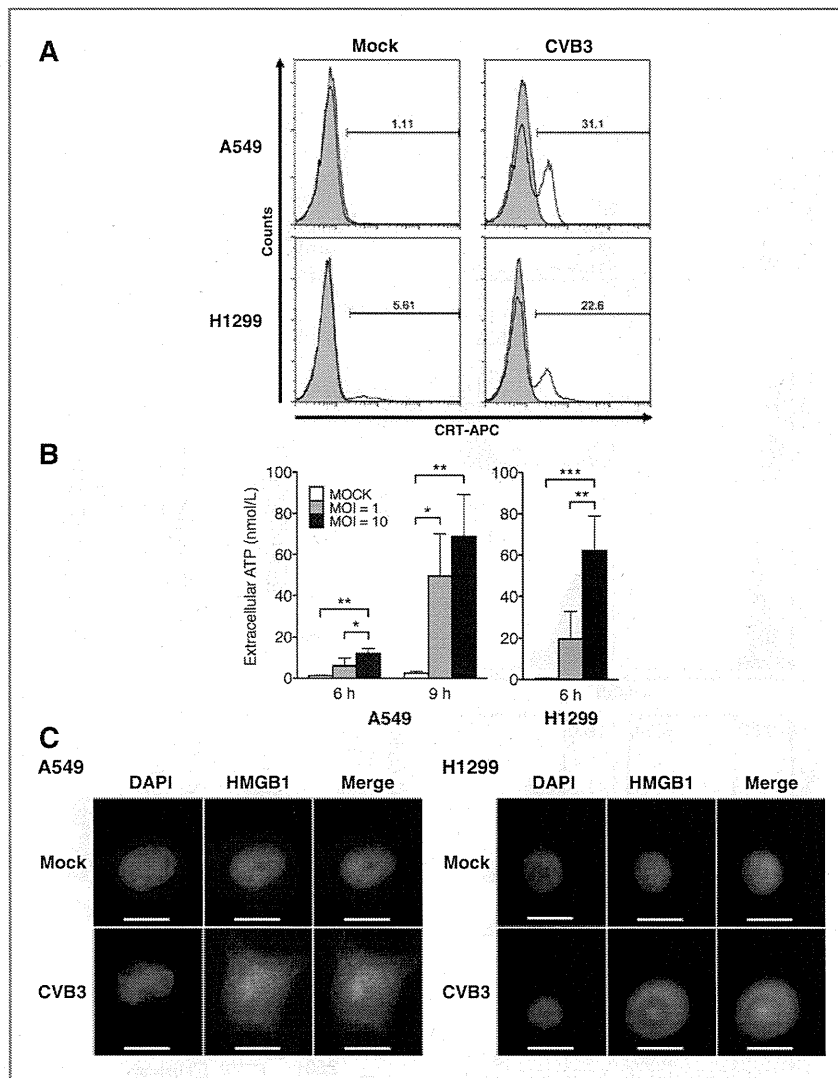


Figure 6. Induced immunogenicity in CVB3-infected NSCLC cells. A, CRT expression on the surface of A549 and H1299 cells was analyzed at 6 hours after CVB3 infection (MOI = 10) by flow cytometric analysis. B, cells were infected with CVB3 at MOI of 1.0 or 10, incubated for 6 or 9 hours, and the concentration of extracellular ATP in the culture medium was measured. Results are shown as means \pm SD. *, $P < 0.05$; **, $P < 0.01$; ***, $P < 0.001$. C, immunofluorescence microscopy images of HMGB1 released from nuclei to cytosol in A549 cells infected with CVB3 for 7 hours. Cells were stained with anti-HMGB1 (green) antibody and DAPI (blue), and analyzed by fluorescence microscopy. Scale bars, 10 μ m.

production from NSCLC cells raises the possibility that the use of PI3K inhibitors might regulate undesired CVB3 replication. The activity of ERK, the downstream target of MEK in the MEK/ERK survival pathway, was also closely correlated with CVB3-mediated cytotoxicity. Enhanced activation of MEK/ERK has been detected in 34% of 111 primary NSCLC patients with lower survival, but not in normal lung tissue (40, 41), providing further insight into the interplay of CVB3 replication with cellular components to improve antitumor efficacies.

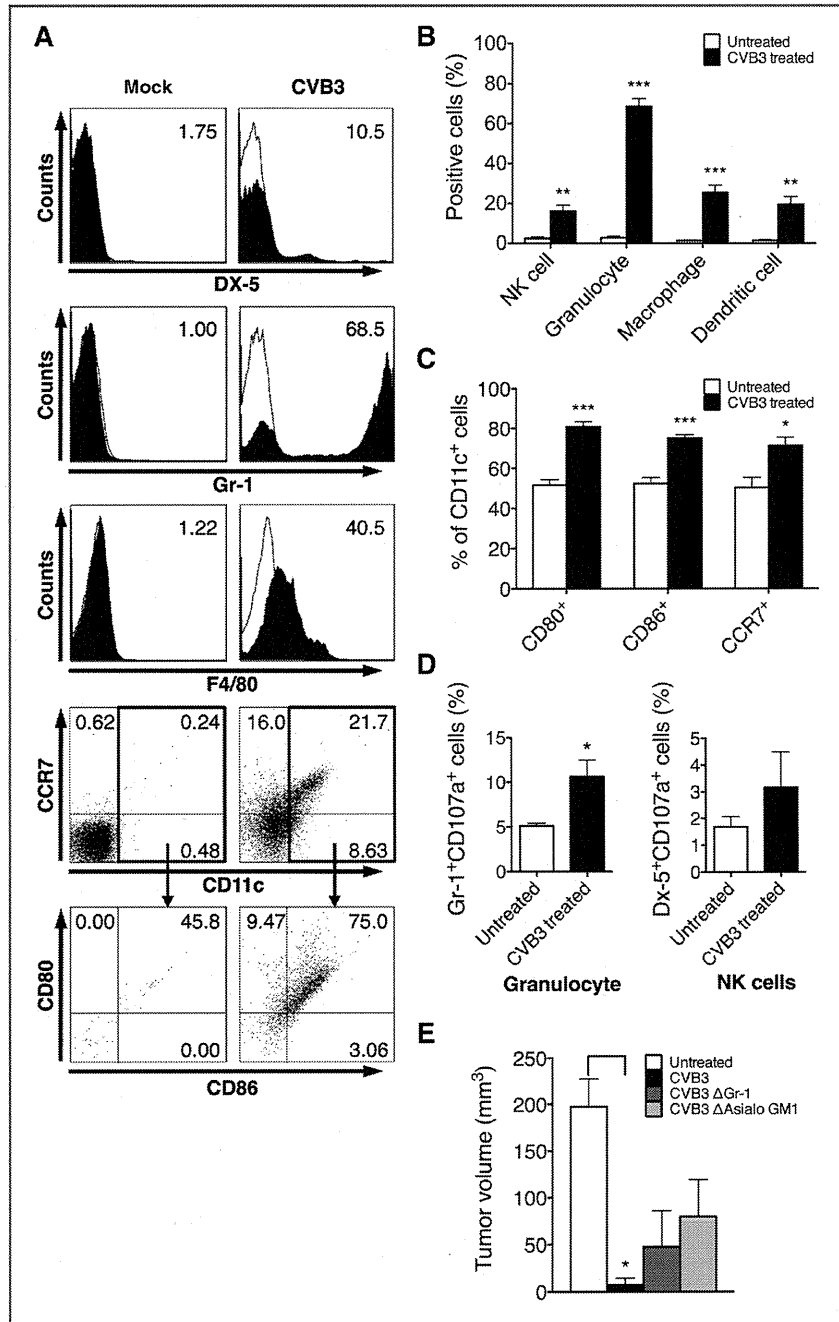
It is noteworthy that intratumoral CVB3 administrations showed significant antitumor effects against A549 adenocarcinoma xenografts resistant to radiotherapy (42) and the EGFR tyrosine kinase inhibitor, gefitinib (43), EBC-1 squamous cell carcinoma (Fig. 5E and F), and H1299 adenocarcinoma xenografts (Supplementary Fig. S3), indicating that CVB3 could be a

favorable therapeutic agent for patients with advanced NSCLC refractory to conventional radiotherapies and/or molecular targeted therapies.

Intratumoral CVB3 administration into one of 2 bilateral subcutaneous xenografts elicited significant suppression of growth of the distant uninjected tumors in which oncolytic CVB3 progeny could be detected. This implies that the administered CVB3 replicated, and its progeny circulated via the blood or lymphatic system and infected distant tumors, which is a beneficial for the systemic treatment of metastatic or disseminated tumors.

For toxicity evaluation, we conducted biochemical and histologic assays during CVB3 treatment. CVB3 administration induced moderate hepatic dysfunction (Supplementary Fig. S4A), with no histologic evidence of active hepatitis

Figure 7. Immunostimulatory effects of intratumoral CVB3 administration on tumor-infiltrating lymphocytes (TIL). TILs obtained on day 2 after intratumoral CVB3 administration were subjected to flow cytometry analysis. **A**, numbers presented in the histogram reflect the percentage of DX-5⁺, Gr-1⁺, F4/80⁺, and CD11c⁺ cells relative to the total cell number of TILs (top 3 rows). The numbers presented in 2-dimensional dot plots reflect the percentage of different mature DC subsets relative to the total number of DCs (bottom 2 rows). **B**, percentages of innate immune subpopulations of NK cells, granulocytes, macrophages, and DCs relative to the total cell count of TILs are shown (*n* = 5). **, *P* < 0.01; ***, *P* < 0.001. **C**, percentages of 3 different subtypes of mature DCs relative to the total count of DCs are shown. Bar graphs depict the means ± SEM (*n* = 5). *, *P* < 0.05; ***, *P* < 0.001. **D**, percentages of granulocytes or NK cells expressing CD107a in enriched TILs relative to total TILs are shown. *, *P* < 0.05. **E**, nude mice (*n* = 4) bearing A549 cells were injected intraperitoneally with anti-Gr-1 antibody on days 1, 4, 7, 10, 13, 16, and 19, or anti-asialo GM1 antibody on days 1, 7, 13, and 19 posttumor challenge. CVB3 virus was injected into the right lateral tumor every other day for a total of 5 doses (5×10^6 TCID₅₀/dose). The tumor volumes measured on day 18 are shown (*n* = 4). *, *P* < 0.05.



(Supplementary Fig. S4B). There have been no reports of human hepatitis caused by CVB3 infection. Elevated creatinine kinase was found in the sera of CVB3-treated mice, with histologic evidence of mild myocarditis, but no cytopathic damage in the lungs or kidneys (Supplementary Fig. S4B). Although human CAR mRNA is expressed in the heart (44),

CVB3 possibly causes severe myocarditis in infants only (45), suggesting its relatively mild side effects in use for adult patients.

As oncolytic virotherapy is expected to promote inflammatory DAMP within the tumor, which is beneficial for effective antitumor immune responses, it is important to assess

whether oncolytic viruses generate immunogenic cell death (18). CVB3 infection induced these immunogenic changes such as CRT exposure, release of extracellular ATP, and HMGB1 translocation in NSCLC cells (Fig. 6). Upon propagation of oncolytic virus, alterations in the repertoire of immune cells in tumor microenvironment can restore inherent antitumor immunity (46), through inductions of interferons and/or cytokines that activate NK cells and mature DCs (47, 48). Tumor-infiltrating DCs have been shown to be impaired at maturation (49). Media from malignant cells infected with reovirus promoted maturation of DCs (46). Likewise CVB3 may alter the immunologic microenvironment by accumulating diverse mature DCs into tumors (Fig. 7C), probably because the single-stranded RNA genome converts dysfunctional DCs into functional DCs after ligation of retinoic acid-inducible gene-1 (RIG-1)-like receptors (50). Indeed, CVB3 intervention was shown to shape NK cell polarization with antitumor effects, possibly through promoted recruitment of cytolytic CD107a⁺ NK cells into xenografts (Fig. 7D and E). Contribution of neutrophils to the antitumor effects may be partially due to IFN- β production following CVB3 administration, as IFN- β can instruct neutrophils to possess an antitumor phenotype (51). These immunostimulatory properties of CVB3 on innate immunity may subsequently prime effective generation of adaptive immunity synergizing with direct oncolytic activities. After showing that TC-1 syngeneic mouse NSCLC cells were susceptible to *in vitro* CVB3 infection (Supplementary Fig. S5A), to further evaluate the effects of T cell-mediated cellular immunity on the oncolytic effects of CVB3, we treated immunocompetent mice with TC-1 tumors with a single CVB3 intratumoral administration, which significantly inhibited TC-1 tumor development in a dose-dependent manner ($P <$

0.05; Supplementary Fig. S5B), with significantly prolonged survival (Supplementary Fig. S5C). These findings indicate that T cell-mediated antiviral immunity is not a significant barrier for intratumoral replication of CVB3.

Notably, in all experiments, no mice manifested lethality during CVB3 treatments, highlighting acceptable safety characteristics as an oncolytic agent.

In summary, our large-scale 2-step screening identified CVB3 as a tumor-specific virus, which depends on apoptotic and survival signaling pathways. Furthermore, systemic and immunostimulatory antitumor effects of CVB3 provide an encouraging avenue for future preclinical and clinical development as a promising viral agent for the treatment of NSCLC patients.

Disclosure of Potential Conflicts of Interest

K. Tani: minor stock, Oncolys BioPharma Inc. No potential conflicts were disclosed by the other authors.

Acknowledgments

The authors thank Michiyo Okada, Michiko Ushijima, and Dr. Shinji Okano (Kyushu University) for technical assistance. The authors also thank the technical support from the Research Support Center, Graduate School of Medical Sciences, Kyushu University.

Grant Support

This work was supported by grants from the Ministry of Education, Culture, Sports, Science and Technology (17016053 and 23240133), and the Ministry of Health Labour and Welfare (23080101), Japan.

The costs of publication of this article were defrayed in part by the payment of page charges. This article must therefore be hereby marked *advertisement* in accordance with 18 U.S.C. Section 1734 solely to indicate this fact.

Received September 23, 2011; revised February 24, 2012; accepted March 14, 2012; published OnlineFirst March 29, 2012.

References

- Russell SJ, Peng KW. Viruses as anticancer drugs. *Trends Pharmacol Sci* 2007;28:326-33.
- Aghi M, Martuza RL. Oncolytic viral therapies—the clinical experience. *Oncogene* 2005;24:7802-16.
- Park BH, Hwang T, Liu TC, Sze DY, Kim JS, Kwon HC, et al. Use of a targeted oncolytic poxvirus, JX-594, in patients with refractory primary or metastatic liver cancer: a phase I trial. *Lancet Oncol* 2008;9:533-42.
- Kumar S, Gao L, Yeagy B, Reid T. Virus combinations and chemotherapy for the treatment of human cancers. *Curr Opin Mol Ther* 2008;10:371-9.
- Morton CL, Houghton PJ, Kolb EA, Gorlick R, Reynolds CP, Kang MH, et al. Initial testing of the replication competent Seneca Valley virus (NTX-010) by the pediatric preclinical testing program. *Pediatr Blood Cancer* 2010;55:295-303.
- Shafren DR, Sylvester D, Johansson ES, Campbell IG, Barry RD. Oncolysis of human ovarian cancers by echovirus type 1. *Int J Cancer* 2005;115:320-8.
- Au GG, Beagley LG, Haley ES, Barry RD, Shafren DR. Oncolysis of malignant human melanoma tumors by Coxsackieviruses A13, A15 and A18. *Virology* 2011;8:22.
- Shafren DR, Au GG, Nguyen T, Newcombe NG, Haley ES, Beagley L, et al. Systemic therapy of malignant human melanoma tumors by a common cold-producing enterovirus, coxsackievirus a21. *Clin Cancer Res* 2004;10:53-60.
- Skelding KA, Barry RD, Shafren DR. Enhanced oncolysis mediated by Coxsackievirus A21 in combination with doxorubicin hydrochloride. *Invest New Drugs* 2012;30:568-81.
- Feuer R, Mena I, Pagarigan R, Sliifka MK, Whitton JL. Cell cycle status affects coxsackievirus replication, persistence, and reactivation *in vitro*. *J Virol* 2002;76:4430-40.
- Evans DJ. Reverse genetics of picornaviruses. *Adv Virus Res* 1999;53:209-28.
- Michos AG, Syriopoulou VP, Hadjichristodoulou C, Daikos GL, Lagona E, Douridas P, et al. Aseptic meningitis in children: analysis of 506 cases. *PLoS One* 2007;2:e674.
- Skelding KA, Barry RD, Shafren DR. Systemic targeting of metastatic human breast tumor xenografts by Coxsackievirus A21. *Breast Cancer Res Treat* 2009;113:21-30.
- Kelly EJ, Hadac EM, Greiner S, Russell SJ. Engineering microRNA responsiveness to decrease virus pathogenicity. *Nat Med* 2008;14:1278-83.
- Diaz RM, Galivo F, Kottke T, Wongthida P, Qiao J, Thompson J, et al. Oncolytic immunovirotherapy for melanoma using vesicular stomatitis virus. *Cancer Res* 2007;67:2840-8.
- Matzinger P. Tolerance, danger, and the extended family. *Annu Rev Immunol* 1994;12:991-1045.
- Prestwich RJ, Errington F, Ilett EJ, Morgan RS, Scott KJ, Kottke T, et al. Tumor infection by oncolytic reovirus primes adaptive antitumor immunity. *Clin Cancer Res* 2008;14:7358-66.
- Zitvogel L, Kepp O, Senovilla L, Menger L, Chaput N, Kroemer G. Immunogenic tumor cell death for optimal anticancer therapy: the cationic exposure pathway. *Clin Cancer Res* 2010;16:3100-4.
- Kuninaka S, Yano T, Yokoyama H, Fukuyama Y, Terazaki Y, Uehara T, et al. Direct influences of pro-inflammatory cytokines (IL-1 β , TNF-

- alpha, IL-6) on the proliferation and cell-surface antigen expression of cancer cells. *Cytokine* 2000;12:8–11.
20. Karber G. 50% end-point calculation. *Arch Exp Pathol Pharmacol* 1931;162:480–3.
 21. Meng X, Nakamura T, Okazaki T, Inoue H, Takahashi A, Miyamoto S, et al. Enhanced antitumor effects of an engineered measles virus Edmonston strain expressing the wild-type N, P, L genes on human renal cell carcinoma. *Mol Ther* 2010;18:544–51.
 22. Tesniere A, Schlemmer F, Boige V, Kepp O, Martins I, Ghiringhelli F, et al. Immunogenic death of colon cancer cells treated with oxaliplatin. *Oncogene* 2010;29:482–91.
 23. Inoue H, Iga M, Xin M, Asahi S, Nakamura T, Kurita R, et al. TARC and RANTES enhance antitumor immunity induced by the GM-CSF-transduced tumor vaccine in a mouse tumor model. *Cancer Immunol Immunother* 2008;57:1399–411.
 24. Inoue H, Iga M, Nabeta H, Yokoo T, Suehiro Y, Okano S, et al. Non-transmissible Sendai virus encoding granulocyte macrophage colony-stimulating factor is a novel and potent vector system for producing autologous tumor vaccines. *Cancer Sci* 2008;99:2315–26.
 25. Shafren DR, Williams DT, Barry RD. A decay-accelerating factor-binding strain of coxsackievirus B3 requires the coxsackievirus-adenovirus receptor protein to mediate lytic infection of rhabdomyosarcoma cells. *J Virol* 1997;71:9844–8.
 26. Esfandiarei M, Luo H, Yanagawa B, Suarez A, Dabiri D, Zhang J, et al. Protein kinase B/Akt regulates coxsackievirus B3 replication through a mechanism which is not caspase dependent. *J Virol* 2004;78:4289–98.
 27. Alter G, Malenfant JM, Altfeld M. CD107a as a functional marker for the identification of natural killer cell activity. *J Immunol Methods* 2004;294:15–22.
 28. Grote D, Cattaneo R, Fielding AK. Neutrophils contribute to the measles virus-induced antitumor effect: enhancement by granulocyte macrophage colony-stimulating factor expression. *Cancer Res* 2003;63:6463–8.
 29. Jemal A, Bray F, Center MM, Ferlay J, Ward E, Forman D. Global cancer statistics. *CA Cancer J Clin* 2011;61:69–90.
 30. Fidias P, Novello S. Strategies for prolonged therapy in patients with advanced non-small-cell lung cancer. *J Clin Oncol* 2010;28:5116–23.
 31. Wang Y, Wang S, Bao Y, Ni C, Guan N, Zhao J, et al. Coxsackievirus and adenovirus receptor expression in non-malignant lung tissues and clinical lung cancers. *J Mol Histol* 2006;37:153–60.
 32. Li L, Spendlove I, Morgan J, Durrant LG. CD55 is over-expressed in the tumour environment. *Br J Cancer* 2001;84:80–6.
 33. Dean M, Fojo T, Bates S. Tumour stem cells and drug resistance. *Nat Rev Cancer* 2005;5:275–84.
 34. Carthy CM, Yanagawa B, Luo H, Granville DJ, Yang D, Cheung P, et al. Bcl-2 and Bcl-xL overexpression inhibits cytochrome c release, activation of multiple caspases, and virus release following coxsackievirus B3 infection. *Virology* 2003;313:147–57.
 35. Martin U, Jarasch N, Nestler M, Rassmann A, Munder T, Seitz S, et al. Antiviral effects of pan-caspase inhibitors on the replication of coxsackievirus B3. *Apoptosis* 2007;12:525–33.
 36. Tang JM, He QY, Guo RX, Chang XJ. Phosphorylated Akt overexpression and loss of PTEN expression in non-small cell lung cancer confers poor prognosis. *Lung Cancer* 2006;51:181–91.
 37. Balsara BR, Pei J, Mitsuuchi Y, Page R, Klein-Szanto A, Wang H, et al. Frequent activation of AKT in non-small cell lung carcinomas and preneoplastic bronchial lesions. *Carcinogenesis* 2004;25:2053–9.
 38. Zhou J, Wulfschlegel J, Zhang H, Gu P, Yang Y, Deng J, et al. Activation of the PTEN/mTOR/STAT3 pathway in breast cancer stem-like cells is required for viability and maintenance. *Proc Natl Acad Sci U S A* 2007;104:16158–63.
 39. Lee HE, Kim JH, Kim YJ, Choi SY, Kim SW, Kang E, et al. An increase in cancer stem cell population after primary systemic therapy is a poor prognostic factor in breast cancer. *Br J Cancer* 2011;104:1730–8.
 40. Vicent S, Garayoa M, Lopez-Picazo JM, Lozano MD, Toledo G, Thunnissen FB, et al. Mitogen-activated protein kinase phosphatase-1 is overexpressed in non-small cell lung cancer and is an independent predictor of outcome in patients. *Clin Cancer Res* 2004;10:3639–49.
 41. Vicent S, Lopez-Picazo JM, Toledo G, Lozano MD, Torre W, Garcia-Corchon C, et al. ERK1/2 is activated in non-small-cell lung cancer and associated with advanced tumours. *Br J Cancer* 2004;90:1047–52.
 42. Guo WF, Lin RX, Huang J, Zhou Z, Yang J, Guo GZ, et al. Identification of differentially expressed genes contributing to radioresistance in lung cancer cells using microarray analysis. *Radiat Res* 2005;164:27–35.
 43. Janmaat ML, Rodriguez JA, Gallegos-Ruiz M, Kruyt FA, Giaccone G. Enhanced cytotoxicity induced by gefitinib and specific inhibitors of the Ras or phosphatidylinositol-3 kinase pathways in non-small cell lung cancer cells. *Int J Cancer* 2006;118:209–14.
 44. Tomko RP, Xu R, Philipson L. HCAR and MCAR: the human and mouse cellular receptors for subgroup C adenoviruses and group B coxsackieviruses. *Proc Natl Acad Sci U S A* 1997;94:3352–6.
 45. Dan M, Chantler JK. A genetically engineered attenuated coxsackievirus B3 strain protects mice against lethal infection. *J Virol* 2005;79:9285–95.
 46. Errington F, Steele L, Prestwich R, Harrington KJ, Pandha HS, Vidal L, et al. Reovirus activates human dendritic cells to promote innate antitumor immunity. *J Immunol* 2008;180:6018–26.
 47. Zhang Y, Chirmule N, Gao GP, Qian R, Croyle M, Joshi B, et al. Acute cytokine response to systemic adenoviral vectors in mice is mediated by dendritic cells and macrophages. *Mol Ther* 2001;3:697–707.
 48. Benencia F, Courreges MC, Conejo-Garcia JR, Mohamed-Hadley A, Zhang L, Buckanovich RJ, et al. HSV oncolytic therapy upregulates interferon-inducible chemokines and recruits immune effector cells in ovarian cancer. *Mol Ther* 2005;12:789–802.
 49. Vicari AP, Chiodoni C, Vaure C, Ait-Yahia S, Dercamp C, Matsos F, et al. Reversal of tumor-induced dendritic cell paralysis by CpG immunostimulatory oligonucleotide and anti-interleukin 10 receptor antibody. *J Exp Med* 2002;196:541–9.
 50. Pichlmair A, Reis e Sousa C. Innate recognition of viruses. *Immunity* 2007;27:370–83.
 51. Jablonska J, Leschner S, Westphal K, Lienenklaus S, Weiss S. Neutrophils responsive to endogenous IFN-beta regulate tumor angiogenesis and growth in a mouse tumor model. *J Clin Invest* 2010;120:1151–64.

From: em.dds.0.297491.c54f03fd@editorialmanager.com

[mailto:em.dds.0.297491.

[c54f03fd@editorialmanager.com](mailto:em.dds.0.297491.c54f03fd@editorialmanager.com)] On Behalf Of DDS Editorial Office

Sent: Friday, March 02, 2012 3:47 PM

To: Kazuhiko Nakamura

Subject: Decision on your manuscript (DDAS9331)

Dear Dr. Kazuhiko Nakamura:

On behalf of the editorial board, we are pleased to inform you that

your

manuscript "CD30 Ligand/CD30 Interaction is Involved in Pathogenesis of

Inflammatory Bowel Disease" (DDAS9331) has been accepted for

publication

in

Digestive Diseases and Sciences.

Should any questions arise during the production phase of your manuscript,

please contact production editor Mohan Kumar at

k.mohankumar@springer.com

or

via www.springer.com/10620

Please remember to always include your manuscript number, DDAS9331, in

all

inquiries about your manuscript.

Thank you for submitting this manuscript to Digestive Diseases and Sciences.

It is papers such as yours that will enhance the excellence of our journal.

Sincerely,

David T. Rubin, MD

Associate Editor

Digestive Diseases and Sciences

Jonathan D. Kaunitz, MD

Editor-in-Chief

Digestive Diseases and Sciences

<DDS-S-11-01738.fdf>

CD30 Ligand/CD30 Interaction is Involved in Pathogenesis of Inflammatory Bowel

Disease

Shinichi Somada, M.D.¹, Hiromi Muta, M.D., Ph.D.^{1,2}, Kazuhiko Nakamura, M.D., Ph.D.²,
Xun Sun, M.D., Ph.D.^{3,4,5}, Kuniomi Honda, M.D.², Eikichi Ihara, M.D., Ph.D.², Hirotada
Akiho, M.D., Ph.D.², Ryoichi Takayanagi, M.D., Ph.D.², Yasunobu Yoshikai, M. D., Ph.D.³,
Eckhard R. Podack, M.D.⁶ and Kenzaburo Tani, M.D., Ph.D.¹

(1) Department of Advanced Molecular and Cell Therapy, Kyushu University Hospital,
Fukuoka, Japan

(2) Department of Medicine and Bioregulatory Science, Graduate School of Medical
Sciences, Kyushu University, Fukuoka, Japan

(3) Division of Host Defense, Research Center For Prevention of Infectious Diseases,
Medical Institute of Bioregulation, Kyushu University, Fukuoka, Japan

(4) Research Center for Advanced Immunology, Kyushu University, Fukuoka, Japan

(5) Institute of Immunology, China Medical University, Shenyang, China

(6) Department of Microbiology and Immunology, University of Miami, Miller School of
Medicine, Miami, FL

E-mail

Shinichi Somada: ssomada@yahoo.co.jp

Hiromi Muta: hmuta@med.kyushu-u.ac.jp

Kazuhiko Nakamura: knakamur@intmed3.med.kyushu-u.ac.jp

Xun Sun: wsunxun@bioreg.kyushu-u.ac.jp

Kuniomi Honda: kuhonda@intmed3.med.kyushu-u.ac.jp

Eikichi Ihara: eikichi@intmed3.med.kyushu-u.ac.jp

Hirotada Akiho: akiho@intmed3.med.kyushu-u.ac.jp

Ryoichi Takayanagi: takayana@intmed3.med.kyushu-u.ac.jp

1 Yasunobu Yoshikai: yoshikai@bioreg.kyushu-u.ac.jp

2 Eckhard R. Podack: EPodack@med.miami.edu

3
4
5 Kenzaburo Tani: taniken@bioreg.kyushu-u.ac.jp

6
7
8
9
10 Word counts: abstract and text 3075

11 Scientific heading: Immunobiology

12
13
14 This work was supported in part by Health and Labour Science Research Grants from the
15
16 Japanese Ministry of Health, Labour and Welfare.

17
18
19
20
21 Corresponding author:

22
23
24 Kazuhiko Nakamura, Department of Medicine and Bioregulatory Science, Graduate School
25
26 of Medical Sciences, Kyushu University, 3-1-1, Maidashi, Higashi-ku, Fukuoka 812-8582,
27
28 Japan

29
30
31 E-mail: knakamur@intmed3.med.kyushu-u.ac.jp

32
33
34 Tel: +81-92-642-5286; Fax: +81-92-642-5287

Abstract

1
2
3
4
5
6
7
8
9
10
11
12
13
14
15
16
17
18
19
20
21
22
23
24
25
26
27
28
29
30
31
32
33
34
35
36
37
38
39
40
41
42
43
44
45
46
47
48
49
50
51
52
53
54
55
56
57
58
59
60
61
62
63
64
65

Background and Aims: Although CD30 has long been recognized as an important marker in many lymphomas of diverse origin, and as an activation molecule on B and T cells, its primary function has remained obscure. Soluble CD30 (sCD30) is released from CD30 on the cell membrane by enzymatic cleavage. This study investigated the role of CD30 ligand (CD30L)/CD30 signals in intestinal mucosal damage. *Methods:* Serum sCD30 in patients with ulcerative colitis (UC) and Crohn's disease (CD) and healthy individuals was assessed. A model of enteritis induced by anti-CD3 monoclonal antibody injection was studied in wild-type mice and in CD30L knockout mice. *Results:* Increased sCD30 was observed in UC and CD patients, and the level was correlated with disease activity in both conditions. In a murine model of enteritis, histological intestinal damage was significantly reduced in CD30L knockout mice with decreased Th1 and Th17 cytokine levels. Moreover, blocking of CD30L/CD30 signals by CD30-immunoglobulin (CD30-Ig) resulted in reduced inflammation. *Conclusions:* Increased sCD30 expression correlating with disease activity suggested that CD30L/CD30 signals play an important role in pathogenesis of UC and CD. CD30L/CD30 pathway acts as an accelerator of enteritis in a murine disease model. Successful blockade of enteritis by CD30-Ig suggests a potential tool for future therapy of inflammatory bowel diseases.

Keywords CD30, CD30 ligand, Inflammatory bowel disease, Ulcerative colitis, Crohn's disease

Introduction

1
2
3 CD30 and CD30 ligand (CD30L) are glycoproteins that belong to the tumor necrosis
4 factor receptor (TNFR) and tumor necrosis factor (TNF) superfamily, respectively [1, 2].
5
6 CD30 is expressed by activated lymphoid and lymph node cells in the parafollicular area,
7
8 decidua, and in endometrial cells with deciduoid changes. The extracellular part of
9
10 membrane-bound CD30 can be proteolytically cleaved by the action of a zinc metalloprotease
11
12 [3], which produces a soluble form of CD30 (sCD30) with a molecular mass of 85/90 kDa.
13
14 Elevated levels of sCD30 have been observed in patients with various diseases such as
15
16 systemic lupus erythematosus, rheumatoid arthritis and human immunodeficiency virus-1
17
18 infection [4]. The source of sCD30 is assumed to be CD30-expressing cells. Although its
19
20 function remains to be clarified, sCD30 can bind to CD30L and block the interaction between
21
22 CD30 and its ligand. CD30L/CD30 signaling is thought to augment T and B cell
23
24 differentiation and proliferation, and negative selection of T cells in the thymus [2, 5–9]. We
25
26 have previously reported that triggering of CD30 signals in a lymphoma cell line can
27
28 down-modulate lymphocyte effector function and proliferation, while directing the cells to
29
30 lymph nodes and increasing their susceptibility to certain apoptotic signals [10]. We have
31
32 constructed CD30L knockout mice (CD30LKO), and have found that CD30L/CD30 signals
33
34 play potent roles in regulation of CD4⁺ T-cell-mediated graft-versus-host disease [11], and in
35
36 the differentiation of long-lived central memory CD8⁺ T cells following infection [12].
37
38
39
40
41
42
43
44
45
46

47 Inflammatory bowel disease (IBD), including ulcerative colitis (UC) and Crohn's
48
49 disease (CD), is of unknown etiology. Recent reports have suggested that chronic
50
51 inflammation occurs as consequence of aberrant intestinal immune responses to the bacterial
52
53 microflora in genetically susceptible individuals [13]. It is believed that T cells, especially T
54
55 helper (Th) cells, play a crucial role in disease development. Some reports have suggested
56
57 that Th cells in the intestinal mucosa in CD are polarized to Th1 and to Th2 in UC [13]. In
58
59
60
61
62
63
64
65

1
2
3
4
5
6
7
8
9
10
11
12
13
14
15
16
17
18
19
20
21
22
23
24
25
26
27
28
29
30
31
32
33
34
35
36
37
38
39
40
41
42
43
44
45
46
47
48
49
50
51
52
53
54
55
56
57
58
59
60
61
62
63
64
65

addition, recent evidence has suggested that a new Th subset, Th17, is implicated in the pathogenesis of CD and UC [14, 15]. As regards the involvement of CD30L/CD30 signaling in IBD, serum sCD30 concentration is elevated in UC but not in CD [16]. We have reported previously [17] that an experimental colitis model induced by oxazolone enema was worsened in CD30LKO mice with increased expression of Th2 cytokines including interleukin (IL)-4 and IL-13. On the contrary, CD30LKO mice were resistant to another experimental colitis by trinitrobenzene sulfonic acid (TNBS) enema, with significant reduction in Th1 cytokine, interferon (IFN)- γ expression. The latter showed the involvement of CD30L/CD30 signaling in Th1-mediated colitis and is inconsistent with the former, which suggests that CD30L/CD30 signals play a role in Th2 responses in UC [16]. We thus considered that many issues remained to be clarified about the role of CD30L/CD30 pathways in the pathogenesis of IBD. To address such issues, we investigated the expression of sCD30 in IBD patients and the effect of inhibiting CD30L/CD30 signals in a murine experimental model of enteritis.

Methods

Patients

All patients in this study were admitted to Kyushu University Hospital, Saiseikai Fukuoka General Hospital, National Fukuoka-Higashi Medical Center, or Harasanshin Hospital between 2003 and 2004. The protocol was approved by the institutional ethical committee at all institutions. Written informed consent was obtained from all patients. We obtained peripheral blood samples from 25 UC patients, 16 CD patients, and 12 hospital employees as control subjects. Nine UC and five CD patients were subjected to examination before and after medical treatment. For diagnosis of UC, all patients underwent colonoscopy and a pathological examination of a colonic biopsy sample, to rule out CD, ischemic colitis,

1 or infectious colitis. The disease activity was scored according to the Rachmilewitz Clinical
2 Activity Index [18]. CD patients underwent colonoscopy and/or X-ray examination of the
3 small intestine, and a diagnosis was made based on the presence of typical longitudinal ulcers
4 and/or a cobblestone appearance, and in some cases, the detection of granuloma by
5 histological examination. UC, ischemic colitis, Behçet's disease, and infectious enterocolitis
6 were all ruled out.
7
8
9
10
11
12
13
14
15
16

17 **Mice**

18
19 BALB/cN Sea mice were purchased from Kyudo (Saga, Japan). CD30LKO mice on a
20 BALB/c background were obtained by backcrossing CD30LKO mice with wild-type (WT)
21 BALB/c mice for more than nine generations [11]. Genotypes of CD30LKO mice were
22 screened by PCR as described previously [11]. All mice were 8–12 weeks of age, housed in a
23 pathogen-free facility, and handled according to the recommended guidelines of the Animal
24 Centre of Kyushu University.
25
26
27
28
29
30
31
32
33
34
35

36 **Reagents**

37
38 Anti-mouse CD3 monoclonal antibody (mAb) (145-2C11) was purchased from R&D
39 Systems (Minneapolis, MN, USA), or purified from culture supernatant of a hybridoma
40 purchased from American Type Culture Collection (Manassas, VA, USA). To produce
41 recombinant protein CD30-immunoglobulin (CD30-Ig), murine CD30 cDNA was truncated
42 at the extracellular domain next to the transmembrane segment (nucleotide 906) and fused to
43 the hinge region of murine IgG1, as described previously [6].
44
45
46
47
48
49
50
51
52
53
54

55 **sCD30**

56 sCD30 concentrations in human serum were determined by a specific ELISA kit
57
58
59
60
61
62
63
64
65

1
2
3
4
5
6
7
8
9
10
11
12
13
14
15
16
17
18
19
20
21
22
23
24
25
26
27
28
29
30
31
32
33
34
35
36
37
38
39
40
41
42
43
44
45
46
47
48
49
50
51
52
53
54
55
56
57
58
59
60
61
62
63
64
65

purchased from Bender Med Systems (Burlingame, CA, USA). sCD30 concentration in mouse serum was determined by a specific ELISA kit (GT, Minneapolis, MN, USA).

Experimental Enteritis Model of Anti-CD3 mAb Injection

Anti-CD3 induced enteritis is a well-established experimental model of T-cell-dependent enteritis in mice [19]. The toxic effects of anti-CD3 antibody are caused by activated CD4⁺ and CD8⁺ effector cells in the gut mucosa. WT and CD30LKO mice were injected i.p. with 100 µg anti-CD3 mAb in 500 µl PBS. After 2, 4, 24 and 72 h, peripheral blood was obtained and analyzed. Body weight was measured every day after injection of anti-CD3 mAb. Mice injected with anti-CD3 mAb were killed 24 h after injection, and the terminal ileum was removed. The tissue sections were stained with hematoxylin and eosin (H&E) and examined by optical microscopy. The occurrence of apoptosis in the ileal section was assessed by TUNEL staining using the *in situ* Apoptosis Detection Kit (Takara Bio, Shiga, Japan)

Cytokine Measurement

Peripheral blood was collected from mice at 2 or 4 h after the injection of anti-CD3 antibodies. Sera were separated by centrifugation (4°C, 200 g, 20 min). TNF-α, IFN-γ, IL-4 and IL-17 concentrations in mouse serum were determined with specific ELISA kits (GT).

Statistical Analysis

Student's *t* test was used for statistical comparisons between two groups. *P* < 0.05 was considered statistically significant.

Results

Expression of CD30 in IBD

1
2
3
4
5
6
7
8
9
10
11
12
13
14
15
16
17
18
19
20
21
22
23
24
25
26
27
28
29
30
31
32
33
34
35
36
37
38
39
40
41
42
43
44
45
46
47
48
49
50
51
52
53
54
55
56
57
58
59
60
61
62
63
64
65

We analyzed sera obtained from 25 UC and 16 CD patients, and 12 healthy volunteers, whose demographics are summarized in Table 1. The levels of sCD30 in UC and CD patients were significantly higher than those in healthy subjects (Fig. 1A). To investigate the relationship between disease activity and sCD30 expression, levels of sCD30 measured before and after treatment were compared in 9 UC and five CD patients (Fig. 1B). Disease activity was reduced in all patients after treatment; similarly, serum levels of sCD30 decreased after treatment in all but one patient with UC. sCD30 levels and clinical scores in UC and CD were assessed and were found to be significantly correlated (Fig. 1C). sCD30 is thought to be generated as a consequence of shedding of CD30 from the membrane of CD30-expressing cells; therefore, these results suggested increased CD30 expression in IBD in association with disease activity.

CD30LKO mice are Resistant to Anti-CD3 Antibody Enteritis

To validate a role for CD30 signals in mucosal immunity, we studied anti-CD3-induced enteritis in WT and CD30LKO mice. In this model, the systemic administration of anti-CD3 induces small bowel inflammation and causes diarrhea, piloerection, and changes in overall mobility [19]. We analyzed levels of serum sCD30 in WT mice by ELISA after injection of anti-CD3 antibody. Serum sCD30 levels increased after anti-CD3 antibody treatment and reached a peak at 24 h (Fig. 2), which suggested upregulation of CD30 expression.

To examine the impact of the absence of CD30 signals on anti-CD3-induced enteritis, changes in body weight of WT and CD30LKO mice were measured daily after administration of anti-CD3 (Fig. 3A). Body weight loss in CD30LKO mice was significantly less than that in WT mice at days 2, 4, 5, 6 and 7, which indicated that the absence of CD30 signals